International Journal of Production Research
2009, 1–21, iFirst

Integrating GD&T into dimensional variation models for multistage machining processes

Jean-Philippe Loose[a], Qiang Zhou[a], Shiyu Zhou[a]* and Darek Ceglarek[b]

[a]*Department of Industrial and Systems Engineering, The University of Wisconsin, Madison, Wisconsin, USA;* [b]*The Digital Laboratory, WMG, University of Warwick, Coventry, CV4 7AL, UK*

(*Received 28 March 2008; final version received 12 December 2008*)

Recently, the modelling of variation propagation in multistage machining processes has drawn significant attention. In most of the recently developed variation propagation models, the dimensional variation is determined through kinematic analysis of the relationships among error sources and dimensional quality of the product, represented by homogeneous transformations of the actual location of a product's features from their nominal locations. In design and manufacturing, however, the dimensional quality is often evaluated using Geometric Dimensioning and Tolerancing (GD&T) standards. The method developed in this paper translates the GD&T characteristic of the features into a homogeneous transformation representation that can be integrated in existing variation propagation models for machining processes. A mathematical representation using homogeneous transformation matrices is developed for position, orientation and form characteristics as defined in ANSI Y14.5; further, a numerical case study is conducted to validate the developed methods.

Keywords: GD&T characteristics; mathematical modelling; variation propagation; machining process; homogeneous transformation matrices

1. Introduction

Geometric and dimensional accuracy is a critical quality characteristic of a product. In practice, the allowable deviations from the part's nominal geometry and dimensions are specified during the design stage by defining tolerances on the part's features using Geometric Dimensioning and Tolerancing (GD&T) standards (ASME 1994). Applied to a workpiece's feature, these tolerances define a zone constraining its allowable variation from nominal location, orientation or shape. GD&T standards provide evaluation criteria for dimensional quality. However, in order to achieve high dimensional quality, it is highly desirable to identify the relationship between the product dimensional quality and process layout and parameters.

Most recently, a group of researchers including the authors developed 'stream of variation' (SOVA) methodologies, which focus on dimensional variation analysis of sequential multistage machining and assembly processes using kinematic analysis of the manufacturing operations (Jin and Shi 1999, Ding *et al.* 2000, Huang *et al.* 2000, Djurdjanovic and Ni 2001, Zhou *et al.* 2003, Huang *et al.* 2007a,b, Loose *et al.* 2007).

*Corresponding author. Email: szhou@engr.wisc.edu

ISSN 0020–7543 print/ISSN 1366–588X online

DOI: 10.1080/00207540802691366
http://www.informaworld.com

Here, a 'multistage' machining process refers to a process in which a part is machined through multiple setups. The 'kinematic analysis' refers to the analysis of the spatial location of a feature on a workpiece after the translation and rotation from its nominal location by using homogeneous transformations. In a multistage machining process, the deviation of the feature location at one stage is caused by both *local errors* at the current stage and the *propagated errors* from previous stages. These SoV models are quite effective in describing the interactions between the product dimensional quality and the errors at different stages. Using the SoV models, quick root cause identification and process design improvement can be further achieved (Ding *et al*. 2002a, 2002b, 2005a, 2005b, Zhou *et al*. 2004, Kong *et al*. 2005). Thus, SoV is a promising methodology for effective control of multistage manufacturing processes. A recent monograph (Shi 2006) and a review paper (Ceglarek *et al*. 2004) provided detailed descriptions of the existing research work on SoV modeling and applications in multistage manufacturing processes.

In the SoV models, the geometric and dimensional errors of a feature, which are the deviations from its nominal location and orientation, are represented using a differential motion vector. Figure 1 illustrates the difference in the error representation between GD&T standard and the vectorial representation used in SoV models. Figure 1(a) shows geometric tolerance zone under GD&T standard with a cylindrical feature and shows the boundaries of the tolerance zone (dotted lines) around the true cylindrical feature (solid line), while Figure 1(b) shows the vectorial representation of the deviation of a cylindrical feature.

In Figure 1(b), the design nominal location and orientation of the cylindrical feature can be represented by a local coordinate system (^{0}LCS) attached to the nominal feature (represented by a dashed line in the figure). The location and orientation of the ^{0}LCS is known in the PCS (part coordinate system) by the homogeneous transformation matrix (HTM) $\mathbf{^0H}$, which represents the coordinate transformation from PCS to ^{0}LCS. The true location and orientation of the cylinder after machining can be represented by another local coordinate system (LCS) attached to the actual feature (represented by a solid line in the figure). Then, the geometric and dimensional errors of this feature can be represented

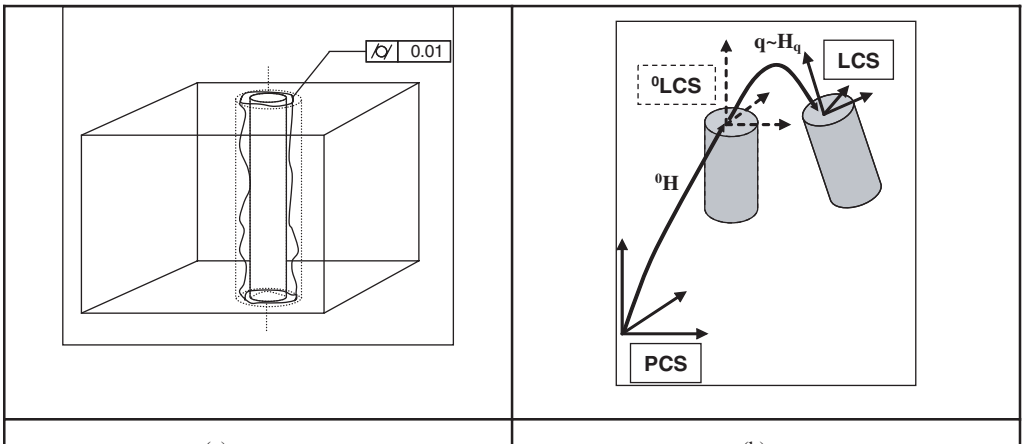

Figure 1. Concept of differential motion vector versus GD&T tolerance.

by a HTM $\mathbf{H_q}$, which represents the transformation from ^{0}LCS to LCS. It needs to be pointed out that although a HTM is a four by four matrix, there are only six independent variables in a HTM, determining three translational and three rotational motions. When the errors are small, $\mathbf{H_q}$ can be approximated by (Paul 1981):

$$\mathbf{H_q} = \begin{bmatrix} 1 & -e_3 & e_2 & x \\ e_3 & 1 & -e_1 & y \\ -e_2 & e_1 & 1 & z \\ 0 & 0 & 0 & 1 \end{bmatrix}. \tag{1}$$

The translational deviation, denoted as $[x, y, z]^T$, and the orientation deviation, denoted as $[e_1, e_2, e_3]^T$, can be collected into a single column matrix called differential motion vector which is associated with $\mathbf{H_q}$ (Paul 1981, Craig 1989):

$$\mathbf{q} = \begin{bmatrix} x & y & z & e_1 & e_2 & e_3 \end{bmatrix}^T. \tag{2}$$

Using the differential motion vector to represent the dimensional quality of a product in SoV models is naturally due to the fact that homogeneous transformation is the fundamental tool in kinematic analysis. However, this vectorial representation of part dimensional quality is different from the GD&T standard currently used during the design phase. Therefore, it is desirable to develop a method to translate the GD&T specification into a HTM representation so that SoV models can incorporate the information of GD&T specification.

GD&T standards provide a generic framework to define the boundaries of the tolerance zones. However, it does not provide a method to obtain them for a specific process. Several methods to mathematically obtain the boundaries representing the tolerance zones have been proposed. Different classifications of these methods can be found in the literature, such as in Requicha (1983), Hong and Chang (2002), or Pasupathy *et al.* (2003). In Pasupathy *et al.* (2003), the authors classify the methods in five groups: (1) offset methods; (2) parametric space methods; (3) algebraic methods; (4) homogeneous transformation methods; and (5) user defined offset zones by parametric curves. For a detailed review of these methods, please refer to the survey by Pasupathy *et al.* (2003). As discussed before, the SoV models utilise homogeneous transformations to describe the feature deviations. Therefore, homogeneous transformation methods are the most relevant methods to incorporate GD&T specifications in the SoV models. Hong and Chang (2002) proposed a classification of homogeneous transformation based methods. Three major directions exist: (1) Rivest *et al.* (1994) proposed to represent the GD&T tolerances using chains of kinematics links; (2) a method based on the use of Jacobian transforms to model the propagation of small deviations along a tolerance chain was developed by Laperrière and Lafond (1998) – this method and the small displacement torsors (SDT) based methods (Bourdet *et al.* 1996, Desrochers 1999, Teissandier *et al.* 1999) are eventually integrated together with the development of a unified method for 3D tolerance analysis (Desrochers *et al.* 2003, Laperrière *et al.* 2003); and (3) 4×4 homogeneous transformation matrices have been used to represent the tolerance zones using parameters for non-invariant displacements in Salomons *et al.* (1996) and Desrochers and Riviere (1997). However, the aforementioned research often does not consider the spatial relationship between controlled features (i.e., features that are subject

to tolerance requirements imposed by GD&T) and the reference datum, and thus does not allow a direct integration of GD&T tolerances into the SoV models.

In this paper, a homogeneous transformation matrix approach is used to represent the boundaries of the dimensional and geometric tolerance zones, taking the reference datum scheme directly into account. Further, the obtained boundaries are utilised to integrate the allowable deviations of the controlled features in the SoV models. A generic procedure is developed and applied to specific GD&T requirements. The relationship between controlled features and reference datums can be directly incorporated in the SoV models when the GD&T tolerances are applied to the controlled features. The detailed mathematical formulation is defined in Section 2. Section 3 presents the complete model derivation for positional, orientation and form tolerances. A case study to illustrate the derivation and validate the results is shown in Section 4. Finally, conclusions and some discussion of the applications are given in Section 5.

2. Review of SoV modelling and problem formulation

2.1 *Brief review of the variation propagation (SoV) model*

In the SoV models, variation propagation in multistage machining processes is modelled following a chain-like state space framework as illustrated in Figure 2 (Zhou *et al*. 2003).

For an N-stage process, the model is in the form of a linear relationship:

$$\mathbf{x}_k = \mathbf{A}_k \mathbf{x}_{k-1} + \mathbf{B}_k \mathbf{e}_k + \mathbf{w}_k, \tag{3}$$

where k is the stage index. The key quality characteristics of the product (e.g., dimensional and geometric deviations of key features) at each stage are represented by the vector $\mathbf{x}_k$. The machining datum errors are incorporated in $\mathbf{x}_k$ and the local process errors at stage k (e.g., fixturing errors) are denoted by $\mathbf{e}_k$. Under small error assumption, $\mathbf{x}_k$ is modelled as a linear function of $\mathbf{x}_{k-1}$ and $\mathbf{e}_k$, where the coefficient matrices $\mathbf{A}_k$ and $\mathbf{B}_k$ are obtained based on the product/process design information, e.g., datum feature selection, the nominal locations of datum features and new features, fixture layout, etc. Therefore, both propagated and local variations are captured in the model. Un-modelled errors in the process are represented by a noise input to the system, noted as $\mathbf{w}_k$. In this paper, we will focus on datum error and fixture error because setup error (datum error in particular) is the key cause of variation propagation in a multistage machining process. Therefore, $\mathbf{w}_k$ includes all other errors such as machine geometric error. As we can see, the complicated variation propagation is handled automatically in the variation propagation model through the state transitions because key quality characteristics of one stage are used as the input for its following stage. Therefore, to construct the model for a multistage machining process, we only need to focus on its local relations between $\mathbf{x}_k$ and $\mathbf{x}_{k-1}$ and $\mathbf{e}_k$ at each stage. The model for the overall process can then be obtained by stacking all stages together. Therefore, in this paper, we will focus on translating the GD&T specifications

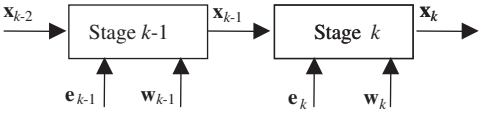

Figure 2. Diagram of a complicated multistage machining process.

into HTM representation at a single stage. Readers might also have noticed that in Equation (3), $\mathbf{x}_k$ is linearly related with $\mathbf{x}_{k-1}$ and $\mathbf{e}_k$. This is due to the fact that in most cases, the geometric and dimensional errors in the system are quite small compared with the nominal dimension of the product and thus a linearised relationship can well approximate the true relationship (Zhou *et al.* 2003). For very large errors such as a broken locator, it is always easy to detect and identify without using the SoV model. Thus, most SoV models adopted the linear structure.

In the SoV model, the state vector $\mathbf{x}_k$ is defined as a stack of *differential motion vectors* (Paul 1981, Craig 1989) that represent the position and orientation deviations of the key features as explained in Figure 1(b). Figures 3(a) and 3(b) also illustrate with a simple single stage machining process the usage of the differential motion vector in the state space model. The machining operation represented by the cutting tool corresponds to the milling of the top surface of a cubic workpiece. The workpiece is mounted on a fixture with a 3-2-1 locating scheme. In this example, the primary datum's dimensional quality (corresponding to the bottom surface of the workpiece) is not ideal (Figure 3(a)). Its inaccuracy is captured by the deviation of the local coordinate system (LCS_A) from its nominal position ($^0LCS_A$) and is denoted by the differential motion vector $\mathbf{q_A}$ on the figure. Because of the dimensional inaccuracy of the primary machining datum, and after the machining operation is carried out, the error will propagate to the feature created at the machining stage (top surface of the workpiece): that feature will not be in its nominal position (Figure 3(b)). Using the linear model shown in Equation (3), the deviation of this feature will be determined in terms of a differential motion vector $\mathbf{q_B}$ representing the deviation from nominal of the coordinate system attached to the top surface (transformation from $^0LCS_B$ to LCS_B).

However, in many cases, the dimensional inaccuracy of machining datum A is not directly given as the deviation of the LCS_A in terms of a differential motion vector. Instead, the most widely used form follows the ANSI GD&T standards. Therefore, there is a need to find an interface between the GD&T characteristics and the SoV model's differential motion vectors.

2.2 *Problem formulation*

The proposed methodology is to transform the GD&T characteristics to corresponding differential motion vectors. First, the scope of the problem needs to be identified. GD&T characteristics can be classified depending on the scale of the corresponding variability.

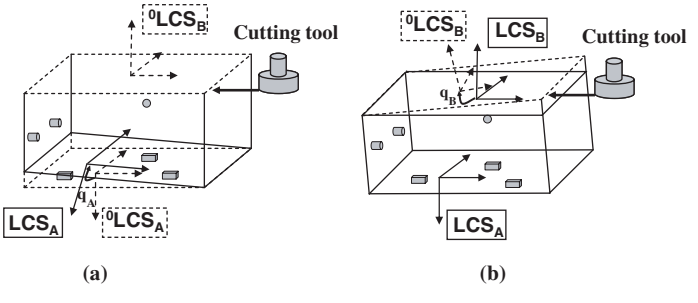

Figure 3. Concept and usage of the state vector.

Henzold (1995) distinguished micro and macro-sources of variations. The micro sources correspond to the surface texture and include surface roughness or waviness. There are four levels of control for macro-variation of a feature defined in GD&T standards: (1) size control; (2) form control; (3) orientation control; and (4) positional control. These levels can be applied to a feature either alone or simultaneously. The first level defines size limits for the controlled feature; the second level controls the overall shape of a feature, described by a boundary inside which the feature must lie. Specifically, there is cylindricity, circularity, flatness or straightness depending on the nominal geometry of the controlled feature. The third level controls the angular relationship of a feature with respect to a different surface, referred to as GD&T reference datum in this paper. There are specific orientation tolerances defined in ANSI Y14.5 as angularity, parallelism, and orthogonality. The fourth level controls both the location and orientation of a feature with respect to a surface. In addition to these three levels, other tolerances such as runout, profile, or symmetry can be defined. However, these additional characteristics can be derived by composing the basic aforementioned control levels. To limit the scope of this paper, we focus on the *analytical modelling and transforming of the macro-variation GD&T characteristics of positional*, *orientation and form*. The rationality of not including micro-sources of variation such as surface texture is that the scale of these errors is between 10 and 100 times smaller than the macro variation sources and their effect on the propagation of dimensional variation can therefore be neglected.

3. GD&T tolerance zone modelling and integration

GD&T characteristics can be defined as either stand-alone or with respect to one or more reference datums. Each characteristic defines a zone in which the controlled feature must lie. The deviation of the controlled feature from nominal in terms of the differential motion vector will be determined and used to represent a realisation of the surface within a zone controlled by a tolerance. In this article, we will determine the *worst case realisations*, corresponding to the largest possible feature deviation achieved without falling outside of its tolerance zone. The corresponding differential motion vector can then be directly used as input to the variation propagation model to represent the feature dimensional inaccuracy in the machining process.

In this paper, we define three types of coordinate systems: (1) the global coordinate system (GCS) is the reference frame; (2) the part coordinate system (PCS) is the reference coordinate system attached to the workpiece; and (3) the local coordinate system (LCS_i, where i represents the index of the feature) is attached to the features of the workpiece. Without loss of generality, the GCS will be defined as the same as the PCS; and LCS_i will always be defined such that its z-direction will be the normal direction of the ith feature at the origin of the LCS_i for a planar feature or the axis of revolution of the ith feature for a conical or cylindrical feature. Also, a notation with a left superscript 0 is used to describe the nominal condition.

3.1 *Model derivation for positional GD&T characteristic*

The primary purpose of positional tolerances is to locate the centre of a feature, such as the centre of a pin or hole. This tolerance is extensively used in engineering drawings; it is

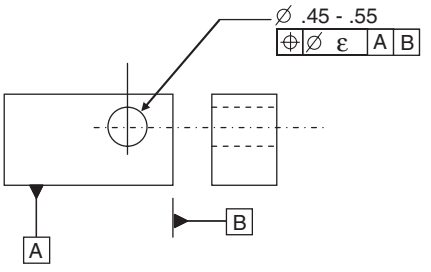

Figure 4. Example of positional tolerance: position of a hole.

defined with respect to one or more datums. The datum(s) will determine the orientation and location of the tolerance zone characterised by the tolerance value ε in which the controlled point or axis can move. Figure 4 shows an example of positional tolerance using two datums.

The nominal location of datums A, B and of the cylinder (feature C) is known in the part coordinate system (PCS): the deviation of the cylinder's centre will be in the plane spanned by the two normal directions to A and B. Without loss of generality, we define the $\mathrm{LCS_C}$ attached to the cylinder so that $(\mathbf{n_A} \times \mathbf{n_B})$ corresponds to the z-direction of the $\mathrm{LCS_C}$, where $\mathbf{n_A}$ and $\mathbf{n_B}$ are the normal directions of datums A and B, respectively. Defining two parameters α_1 and α_2, we can determine:

$$\mathbf{H_q} = \begin{bmatrix} 1 & 0 & 0 & \alpha_1 \\ 0 & 1 & 0 & \alpha_2 \\ 0 & 0 & 1 & 0 \\ 0 & 0 & 0 & 1 \end{bmatrix}, \quad \text{with} \quad \begin{cases} -\dfrac{\varepsilon}{2} \le \alpha_1 \le \dfrac{\varepsilon}{2} \\ -\dfrac{\varepsilon}{2} \le \alpha_2 \le \dfrac{\varepsilon}{2} \\ |\alpha_2| \le \sqrt{\dfrac{\varepsilon^2}{4} - \alpha_1^2} \end{cases}, \tag{4}$$

where $\mathbf{H_q}$ corresponds to the homogeneous transformation matrix associated with the differential motion vector $\mathbf{q} = [\alpha_1 \; \alpha_2 \; 0 \; 0 \; 0 \; 0]^T$ as explained in Figures 1 and 3. $\mathbf{H_q}$ represents the homogeneous transformation matrix of the transformation of the centre or axis from its nominal position to its true position and therefore captures the positional error of the controlled feature. The inequalities in Equation (4) assure that the true feature lies within the tolerance zone. In particular, the third equation in Equation (4) accounts for the circular shape of the positional tolerance zone. Although two of the three inequalities are sufficient to constrain the parameters, the third equation is listed for clarity purpose. By varying the variables α_1 while maximising the variable α_2, it is easy to determine a worst case realisation of $\mathbf{q}$, corresponding to a worst case deviation of the controlled feature.

3.2 *Model derivation for orientation of GD&T characteristics*

We first use parallelism as an example to illustrate the basic idea. Figure 5(a) shows a 3-D workpiece with a parallelism requirement defined on a feature (feature C) with respect to a GD&T reference datum (datum A). In Figure 5(b), the dotted lines represent the nominal conditions; the dashed and dotted lines represent the tolerance zone determined with respect to the GD&T reference datum A; and the solid lines represent the true features. Also, in Figure 5, coordinate systems have been attached on each feature.

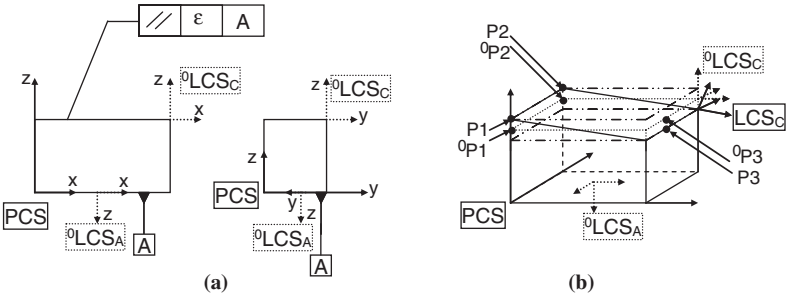

Figure 5. Engineering drawing and true workpiece for a parallelism requirement.

The controlled feature is deviated within the tolerance zone; therefore, each point on the feature will be deviated accordingly. Every point's deviation will be constrained by the tolerance value of the GD&T characteristic. In other words, if we define a point ^0P_i on the nominal feature, it will be deviated by a distance α_i. The value of the parameter α_i is constrained by the GD&T tolerance value. Further, the tolerance zone is defined with respect to GD&T reference datum(s). Therefore the direction of the deviation of the points ^0P_i will depend on the position of the GD&T reference datum.

Since each point on the surface may be deviated and their deviation is parameterised in terms of the GD&T characteristic, the deviation of the entire feature can be determined by a differential motion vector satisfying mathematically that each deviated point should lie on the true feature. The deviation of the feature, expressed in terms of a differential motion vector, can therefore be parameterised by the deviation α_i of the points that constitute the surface. The extreme values of the components of the differential motion vector can be determined through optimisation subject to the constraint that the deviation of each point on the surface should satisfy the GD&T requirement. The extreme values of the differential motion vector correspond physically to a worst case realisation of the feature's geometry and can be directly incorporated into a SoV model.

Based on the above idea, Figure 6 summarises the general procedure for the integration of geometric tolerances in the variation propagation models.

Each step of the proposed methodology is discussed in detail below:

S1. Identify the boundary points on the controlled feature: In this step, N points will be defined on the feature. Assuming rigid parts, the deviation of three points (later referred to as *deviation points*) can be used in 3-D to parameterise the deviation of the entire feature. Therefore, N has to be greater or equal to 3. For $N > 3$, any three of the N points will be used as deviation points. The $N-3$ remaining points will be used as constraints to ensure that the feature lies within the tolerance zone. These points will be referred to as *control points* in the remainder of the paper. A good selection of N points will represent the entire surface of the controlled feature. For example, a set of N points on the surface chosen such that the polygon created by the N points is the convex hull of the vertices of the feature is a good set of points to represent the controlled feature;

S2. Determine the possible positions of the boundary points with respect to the GD&T reference datum(s) in terms of parameters (α_i) representing their deviations;

S3. Determine the possible positions of the boundary points with respect to the nominal feature in terms of the deviation of the LCS attached to the controlled feature

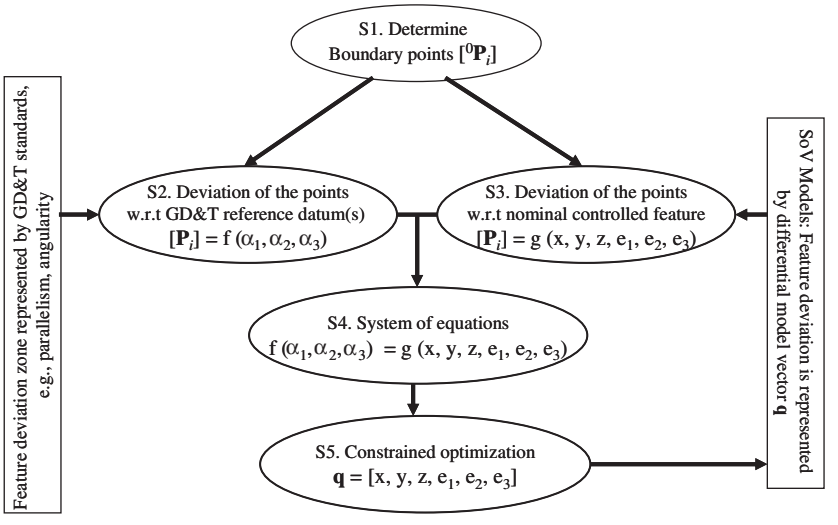

Figure 6. General methodology for incorporating GD&T tolerances in SoV models.

(the location deviation is denoted as $[x\ y\ z]^T$, and the orientation deviation is denoted as $[e_1\ e_2\ e_3]^T$);

S4. Determine the equations linking the deviation of the boundary points to the deviation of the feature by equalising the positions of the points determined in steps S2 and S3 of the procedure; after selecting three deviation points, solve the system to obtain the deviation of the LCS as a function of the individual deviation α_i of the deviation points;

S5. Given the objective of determining the maximum or minimum of one or more components of the differential motion vector representing the deviation of the feature, proceed with the optimisation procedure, subject to the constraint that all boundary points (three deviation points and $N-3$ control points) must lie within the tolerance zone. In other words, the constraints of the optimisation problem are determined by ensuring that the deviations α_i of all N boundary points satisfy the GD&T characteristic. The resulting differential motion vector, corresponding to a worst case realisation of the controlled feature, can be integrated with the variation propagation models.

Clearly, steps S2 and S3 of the procedure are critical steps in the translation of various GD&T characteristics. Two lemmas are introduced as follows to address these two steps.

Lemma 1: *As shown in Figure* 7, *the nominal and true positions of a planar feature* K *are represented by coordinate systems* $^0\mathrm{LCS_k}$ *and* $\mathrm{LCS_K}$, *respectively. Without loss of generality, we assume that the z-axis of* $\mathrm{LCS_K}$ *is the normal direction of the true feature* K. *The matrices* $^0\mathbf{H_K}$, $\mathbf{H_K}$, $\mathbf{H(q_K)}$ *are the homogeneous transformation matrices between* PCS *and* $^0\mathrm{LCS_K}$, PCS *and* $\mathrm{LCS_K}$, $^0\mathrm{LCS_K}$ *and* $\mathrm{LCS_K}$, *respectively. Given two points* $^0\mathrm{P}_i$ *and* $^0\mathrm{P}_{i,\mathrm{true}}$ *that have the same coordinates in* $^0\mathrm{LCS_K}$ *and* $\mathrm{LCS_K}$, *respectively. If the point* $^0\mathrm{P}_{i,\mathrm{true}}$ *is deviated along*

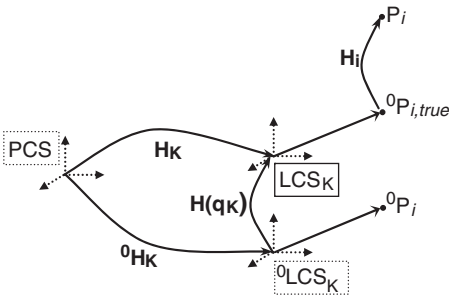

Figure 7. Coordinate systems and homogeneous transformation matrices in Lemma 1.

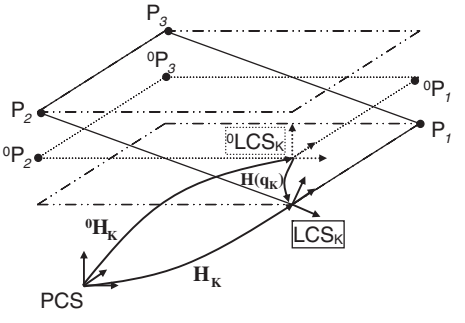

Figure 8. Coordinate systems and homogeneous transformation matrices in Lemma 2.

the normal direction of true feature K *by a distance* α_i *to a new point* P_i, *then the coordinates of* P_i *in* PCS, *denoted as* $\mathbf{P_i}$, *are given by*:

$$\begin{bmatrix} \mathbf{P_i}^T & 1 \end{bmatrix}^T = {}^0\mathbf{H_K} \cdot \mathbf{H}(\mathbf{q_K}) \cdot \mathbf{H_i} \cdot {}^0\mathbf{H_K}^{-1} \cdot \begin{bmatrix} {}^0\mathbf{P_i}^T & 1 \end{bmatrix}^T, \tag{5}$$

where ${}^0\mathbf{P_i}$ *is the coordinate of* ${}^0P_i$ *in the* PCS *coordinate system, and where*:

$$\mathbf{H_i} = \left[\begin{array}{c|c} \mathbf{I}_3 & [0 \quad 0 \quad \alpha_i]^T \\ \hline 0 & 1 \end{array}\right].$$

The proof of this lemma is given in Appendix 1.

Essentially, this lemma provides a method to identify the tolerance zone in PCS when the tolerance zone is identified by deviating points on a feature along the normal direction of a non-ideal datum feature (i.e., feature K in the lemma).

Lemma 2: *As shown in Figure* 8, *the nominal and true positions of a planar feature* K *are represented by coordinate systems* ${}^0LCS_K$ *and* LCS_K, *respectively. The matrices* ${}^0\mathbf{H_K}$, $\mathbf{H_K}$, $\mathbf{H(q_K)}$ *are the homogeneous transformation matrices between* PCS *and* ${}^0LCS_K$, PCS *and* LCS_K, ${}^0LCS_K$ *and* LCS_K, *respectively and* $\mathbf{q_K}$ *is the differential motion vector associated with the homogeneous transformation matrix* $\mathbf{H(q_K)}$. *Given two points* ${}^0P_i$ *and* P_i *that have the*

same coordinates in ${}^0\mathrm{LCS_K}$ *and in* $\mathrm{LCS_K}$, *respectively*, *then their coordinates in* PCS, *denoted as* $\mathbf{{}^0P_i}$ *and* $\mathbf{P_i}$, *satisfy*,

$$\begin{bmatrix} \mathbf{P_i}^T & 1 \end{bmatrix}^T = {}^0\mathbf{H_K} \cdot \mathbf{H(q_K)} \cdot {}^0\mathbf{H_K^{-1}} \cdot \begin{bmatrix} {}^0\mathbf{P_i}^T & 1 \end{bmatrix}^T. \quad (6)$$

The proof is straightforward. Because ${}^0P_i$ has the same coordinates in ${}^0\mathrm{LCS_K}$ as P_i in $\mathrm{LCS_K}$, ${}^0\mathbf{H_K^{-1}} \cdot [{}^0\mathbf{P_i}^T\ 1]^T$ gives the coordinates of P_i in $\mathrm{LCS_K}$. Further left multiplication by ${}^0\mathbf{H_K} \cdot \mathbf{H(q_K)}$ translates the coordinates in $\mathrm{LCS_K}$ into the coordinates in PCS. This lemma essentially provides a method to determine the coordinates of points on a deviated feature (e.g., feature K in the lemma) whose deviation is represented by a differential motion vector $\mathbf{q_K}$.

3.2.1 *Transformation of parallelism characteristic*

In the following, the transformation of parallelism requirement is presented using the abovementioned steps.

S1–S2. Given a workpiece on which one feature has a parallelism requirement with respect to one datum as shown in Figure 5(a), N boundary points are defined on the nominal controlled feature: ${}^0P_1, {}^0P_2, \ldots, {}^0P_N$. Their nominal position is known in the PCS as $\mathbf{{}^0P_i}$, where i is the index of the point. Each of the points can move in the tolerance zone defined with respect to GD&T reference datum A; in other words, for the parallelism requirement, the tolerance zone can be obtained by deviating the points in the normal direction of GD&T reference datum A within an allowable range. Denoting $\mathbf{P_i}$ as the deviated position of boundary point i, then the goal of this step is to express $\mathbf{P_i}$ as a function of the nominal position $\mathbf{{}^0P_i}$ of the boundary point i and its deviation in the normal direction of datum A, denoted as α_i. With this function, the tolerance zone can be identified by constraining the range of α_i; for example, for parallelism, we have: $-\varepsilon/2 \le \alpha_i \le \varepsilon/2$, where ε is the value of the parallelism requirement. The function can be easily obtained using Lemma 1. Treating datum feature A as feature K and $\mathbf{q_A}$, the differential motion vector that represents the deviation of the datum feature, as $\mathbf{q_K}$ in Lemma 1, then Equation (5) provides the coordinates of the deviated boundary points in PCS.

S3. The coordinates of the deviated boundary points can also be obtained using the result of Lemma 2 by deviating feature C. Treating feature C as feature K and $\mathbf{q_C}$, the differential motion vector that represents the deviation of feature C, as $\mathbf{q_K}$ in Lemma 2, then Equation (6) provides the coordinates of the deviated points in PCS.

S4. Steps S2 and S3 give the coordinates of the same set of points in PCS. Thus, by equalising the set of equations for each point, the relationship between the feature deviation represented by differential motion vector and the allowable deviation specified by the GD&T requirement can be established.

Because multiple boundary points are selected, multiple equations can be obtained. For a planar feature, three points are needed to determine the feature's spatial location. The equations derived for the $N-3$ remaining points can be used as constraints to ensure that all boundary points lie within the tolerance zone defined by the GD&T specification.

S5. Finding the extremes of one or more of the components in the differential motion vector $\mathbf{q}$ physically corresponds to calculating the parameters associated with

a worst realisation of the controlled feature within the tolerance zone. Depending on the quality characteristic of interest, the objective function for the constrained optimisation is determined. For the parallelism characteristic, the dimensional quality characteristics of interest are the maxima and minima of each of the individual orientation parameters. The objective function can therefore be defined as $\max(e_1)$, $\min(e_1)$, $\max(e_2)$ or $\min(e_2)$. The deviated feature must lie within the tolerance zone. Hence, the individual boundary points, selected to represent the surface, are constrained by the value of the GD&T characteristic. Assume $N > 3$ boundary points are selected and the first three points are used to establish the relationship between $\mathbf{q_C}$ and α_1, α_2, and α_3, the optimisation problem for e_1 can be finally formalised as:

$$\begin{aligned} &\max && e_1 = g(\alpha_1, \alpha_2, \alpha_3) \\ &\text{subject to :} && \\ &&& \left.\begin{aligned} \alpha_i &\le \frac{\varepsilon}{2} \\ \alpha_i &\ge -\frac{\varepsilon}{2} \end{aligned}\right\}, \qquad \forall i \in (1, \ldots, N) \\ &&& \alpha_j = f_j(\alpha_1, \alpha_2, \alpha_3), \quad \forall j \in (4, \ldots, N), \end{aligned} \tag{7}$$

where g and f_j are linear functions, ε is the value of the GD&T characteristic. The function g is obtained based on the first three points and the functions f_j are obtained with the remaining points and the relationship between $\mathbf{q_C}$ and α_1, α_2, and α_3.

3.2.2 *Transformation of angularity and perpendicularity*

The same procedure can be applied to the transformation of angularity and perpendicularity requirements.

S1–S2. Given a workpiece on which one feature (feature C) has an angularity requirement with respect to two reference datums (datums A and B) as shown in Figure 9.

N boundary points are defined on the nominal controlled feature, ${}^0\mathrm{P}_1, {}^0\mathrm{P}_2, \ldots, {}^0\mathrm{P}_N$. Their nominal position is known in the PCS as $\mathbf{{}^0P_i}$. Each of the points can move in the tolerance zone defined with respect to GD&T reference datums A and B; in other words, each of the points will move in the direction defined by a normal vector to reference datum A rotated by an angle θ around a normal vector to reference datum B. First, the direction

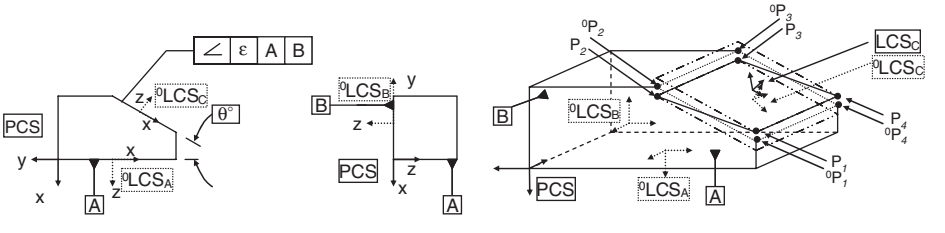

Figure 9. Angularity of a feature.

of the deviation of the points is determined by rotating ${}^0\mathrm{LCS_A}$. Then, the deviated points known in the PCS as $\mathbf{P_i}$ can be calculated using Lemma 1.

Defining ${}^0\mathrm{LCS_A}$, $\mathrm{LCS_A}$, ${}^0\mathrm{LCS_B}$ and $\mathrm{LCS_B}$, determined from the PCS by the homogeneous transformation matrices $\mathbf{{}^0H_A}$, $\mathbf{H_A}$, $\mathbf{{}^0H_B}$ and $\mathbf{H_B}$, respectively, such that the z-directions of ${}^0\mathrm{LCS_A}$ and ${}^0\mathrm{LCS_B}$ are the normal directions of the nominal datums A and B, respectively, the vector $\mathbf{u}$ corresponding to the z-direction of $\mathrm{LCS_B}$ expressed in $\mathrm{LCS_A}$ can be determined as:

$$\begin{bmatrix}\mathbf{u} & 0\end{bmatrix}^T = \mathbf{H_A^{-1}} \cdot \mathbf{H_B}\begin{bmatrix}0 & 0 & 1 & 0\end{bmatrix}^T. \tag{8}$$

Knowing $\mathbf{u}$, $\mathrm{LCS_A}$ can then be rotated by an angle θ specified by the geometry of the workpiece. The rotated $\mathrm{LCS_A}$, called $\mathrm{LCS_G}$ in the following, with its associated homogeneous transformation matrix $\mathbf{H_G}$ from the PCS has its z-axis perpendicular to the tolerance zone. We have:

$$\mathbf{H_G} = \mathbf{H_A} \cdot \mathbf{R}, \tag{9}$$

where $\mathbf{R}$ corresponds to the homogeneous transformation matrix that rotates a coordinate system of an angle θ around an axis defined by a vector $\mathbf{u} = [u_x\ u_y\ u_z]^T$ (Craig 1989):

$$\mathbf{R} = \begin{bmatrix} 1+(1-\cos\theta)\left(u_x^2-1\right) & (1-\cos\theta)u_xu_y - u_z\cdot\sin\theta & (1-\cos\theta)u_xu_z + u_y\cdot\sin\theta & 0 \\ (1-\cos\theta)u_xu_y + u_z\cdot\sin\theta & 1+(1-\cos\theta)\left(u_y^2-1\right) & (1-\cos\theta)u_yu_z - u_x\cdot\sin\theta & 0 \\ (1-\cos\theta)u_xu_z - u_y\cdot\sin\theta & (1-\cos\theta)u_yu_z + u_x\cdot\sin\theta & 1+(1-\cos\theta)\left(u_z^2-1\right) & 0 \\ 0 & 0 & 0 & 1 \end{bmatrix}. \tag{10}$$

Given the deviations in the z-direction of $\mathrm{LCS_G}$ of the boundary points defined as $\alpha_1, \alpha_2, \ldots, \alpha_N$, the coordinates of the deviated boundary points in PCS can be determined using Lemma 1 (Equation (5)), treating $\mathrm{LCS_G}$ as $\mathrm{LCS_K}$:

$$\begin{aligned}\begin{bmatrix}\mathbf{P_i}^T & 1\end{bmatrix}^T &= \mathbf{H_G}\cdot\mathbf{H_i}\cdot\mathbf{H_G^{-1}}\cdot\mathbf{{}^0H_A}\cdot\mathbf{H}(\mathbf{q_A})\cdot\mathbf{{}^0H_A^{-1}}\cdot\begin{bmatrix}\mathbf{{}^0P_i}^T & 1\end{bmatrix} \\ &= \mathbf{H_G}\cdot\mathbf{H_i}\cdot\mathbf{R}^{-1}\cdot\mathbf{{}^0H_A^{-1}}\cdot\begin{bmatrix}\mathbf{{}^0P_i}^T & 1\end{bmatrix},\end{aligned} \tag{11}$$

where $\mathbf{H_i}$ is given in Lemma 1. To ensure that the controlled feature lies within the tolerance zone, the deviations, noted as $\alpha_1, \alpha_2, \ldots, \alpha_N$, for points $\mathrm{P}_1, \mathrm{P}_2, \ldots, \mathrm{P}_N$, respectively, must satisfy $-\varepsilon/2 \le \alpha_i \le \varepsilon/2$, $i = 1, \ldots, N$.

The procedure developed for the angularity characteristics can also be applied to a perpendicularity characteristic by defining an angle $\theta = \pi/2$ of rotation of the normal direction of reference datum A around the normal direction of reference datum B.

The following steps of the transformation of angularity or perpendicularity characteristics are very similar to those of the parallelism characteristic. In step S3, the coordinates of the deviated boundary points given the deviation of the controlled feature C, which is expressed by the differential motion vector $\mathbf{q_C} = [x\ y\ z\ e_1\ e_2\ e_3]^T$ can be obtained using Lemma 2 (Equation (6)). In step S4, by equalising the first three equations obtained in step S2 and step S3, $\mathbf{q_C}$ can be expressed as a function of α_1, α_2, and α_3.

In step S5, the worst case deviation of the controlled feature is obtained by optimising one or more components of the differential motion vector. The dimensional quality of

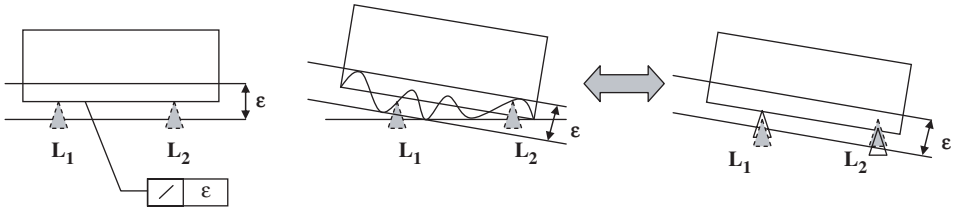

Figure 10. Example of form tolerance: straightness of a line.

interest corresponds to the two orientation parameters; the objective function can therefore be expressed as max(e_1), min(e_1), max(e_2) or min(e_2), etc.

Similar to the parallelism case, the deviated feature must lie within the tolerance zone; therefore, a constrained optimisation problem can be formulated.

3.3 *Transformation for form GD&T characteristics*

In GD&T standards, the form tolerance is defined to obtain a tolerance zone in which the controlled feature is free to be deformed. Specific characteristics are defined given the nominal geometry of the controlled feature: straightness of a 2-D line, flatness of a 3-D plane, etc. The tolerance zone is obtained by offsetting each point on the surface from half of the tolerance value on each side of the nominal feature. If we define points on the surface that are far apart, each point can freely move along the normal direction to the nominal controlled feature constrained by the tolerance zone. By taking points apart, any constraint of continuity of the surface is eliminated. Figure 10 shows an example of form characteristic: the straightness of a line. In this example, the workpiece is a 2-D square, where one of its sides is used as primary datum when the workpiece is mounted in a fixture (the fixture is represented with the locating points L_1 and L_2 in Figure 10).

With this example, it is clear that the deviation of the workpiece due to the form requirement can be expressed by considering the feature with a perfect geometry and with the locators having a deviation along the normal direction of the controlled feature at the point of contact with the locator. It is therefore easy to incorporate form tolerances in the SoV models by treating form tolerances as an independent fixture error on each locator (corresponding to the local error $\mathbf{e}_k$ in Equation (3)). The locators will be deviated along the normal direction of the surface at the contact point within $\pm$ half of the form tolerance value.

4. Experimental validation

The developed technique for transforming the GD&T characteristics applied on a controlled feature into the corresponding feature deviation represented by differential motion vector is validated on a machining process. In this section we first introduce the process; then the variation propagation model is developed, and finally results are validated.

Table 1. Nominal position of the LCS.

Feature	Notation	$[x \quad y \quad z \quad \phi \quad \upsilon \quad \psi]$
$A \sim {}^0LCS_A$	${}^0H_A$	$[52.5566 \quad 1.4805 \quad 0 \quad \pi/2 \quad 0 \quad 0]^T$
$B \sim {}^0LCS_B$	${}^0H_B$	$[0 \quad -25.98072 \quad 25 \quad 0 \quad 0 \quad 0]^T$
$C \sim {}^0LCS_C$	${}^0H_C$	$[0 \quad 0 \quad 0 \quad 0 \quad \pi/2 \quad -\pi/6]^T$
$D \sim {}^0LCS_D$	${}^0H_D$	$[67.556644 \quad 16.480547 \quad 20 \quad -\pi/2 \quad \pi/2 \quad \pi/2]^T$
$f_1 \sim {}^0LCS_{f1}$	${}^0H_1$	$[37.5 \quad 30.31088 \quad 25 \quad 0 \quad -\pi/2 \quad -\pi/6]^T$

Table 2. Nominal position of the locators.

Feature	Locator	Coordinates	Normal direction
C	L_1	$[3.75 \quad -2.1650 \quad -12.5]^T$	$[-0.5 \quad -0.866 \quad 0]^T$
C	L_2	$[-3.75 \quad 2.1650 \quad 12.5]^T$	$[-0.5 \quad -0.866 \quad 0]^T$
C	L_3	$[-11.25 \quad 6.495 \quad -2.5]^T$	$[-0.5 \quad -0.866 \quad 0]^T$
E	L_4	$[0 \quad 25.98 \quad 25]^T$	$[0 \quad 0 \quad 1]^T$
E	L_5	$[7.5 \quad 12.99 \quad 25]^T$	$[0 \quad 0 \quad 1]^T$
A	L_6	$[67.5566 \quad 36.4805 \quad 0]^T$	$[1 \quad 0 \quad 0]^T$

4.1 *Introduction to the machining process*

The following machining process is adapted from a real machining process with modifications due to confidentiality considerations. It is a one stage process and one feature will be machined on the workpiece through milling.

The machining operation consists of milling feature f_1. Datums C, E, and A are the primary, secondary and tertiary machining datums of this operation, respectively. Clearly, this fixture layout is not a traditional 3-2-1 layout since the datums are not orthogonal to each other. Therefore, we will use the methodology developed in Loose *et al.* (2007) to create the SoV model. First, coordinate systems are defined on each feature. Table 1 gathers the nominal locations ($[x \; y \; z]$) and orientations ($[\phi \; \upsilon \; \psi]$) of the local coordinate systems with respect to the PCS, following the Euler angular notation for the orientations (Paul 1981).

The nominal location of the locators, expressed in PCS (in this case, we take GCS the same as PCS for the sake of simplicity), are given in Table 2. Table 2 also lists the normal direction of the datum at the points of contact with the locator, expressed in PCS.

Two GD&T tolerances are defined: the first is a perpendicularity characteristic and is defined on machining datum A with respect to GD&T reference datums B and D; the second is an angularity characteristic defined on machining datum C with respect to GD&T reference datums A and B. Also, four boundary points are defined on each feature, as shown in Figure 11. Their coordinates in PCS are given in Table 3.

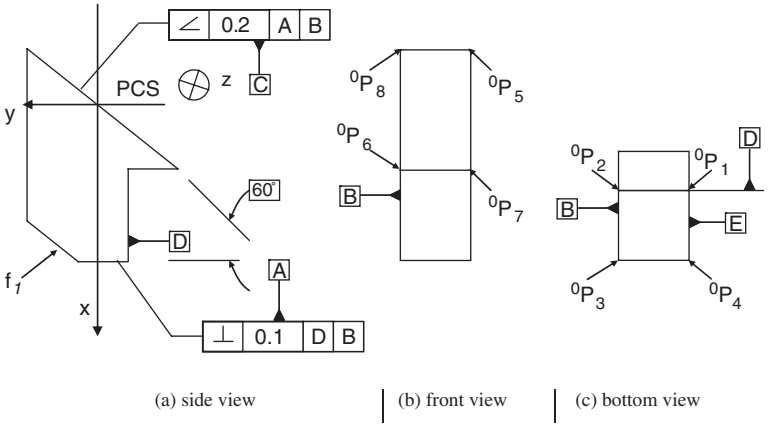

Figure 11. Workpiece for the case study.

Table 3. Nominal position of the locators.

Feature	Point	Coordinates	Feature	Point	Coordinates
A	${}^0P_1$	$[67.55 \quad 1.48 \quad -25]^T$	C	${}^0P_5$	$[-37.5 \quad 21.65 \quad 25]^T$
A	${}^0P_2$	$[67.55 \quad 51.48 \quad -25]^T$	C	${}^0P_6$	$[-37.5 \quad 21.65 \quad -25]^T$
A	${}^0P_3$	$[67.55 \quad 1.48 \quad 25]^T$	C	${}^0P_7$	$[37.5 \quad -21.65 \quad 25]^T$
A	${}^0P_4$	$[67.55 \quad 51.48 \quad 25]^T$	C	${}^0P_8$	$[37.5 \quad -21.65 \quad -25]^T$

4.2 *Determination of the deviation of feature f_1*

Following the procedure in Loose *et al.* (2007), a variation propagation model in the form of Equation (3) is obtained for the machining process with $\mathbf{x_0} = [\mathbf{q_C}\ \mathbf{q_C}\ \mathbf{q_C}\ \mathbf{q_E}\ \mathbf{q_E}\ \mathbf{q_A}]$ and $\mathbf{x_1} = [\mathbf{q_{f_1}}]$, and the coefficient matrices $\mathbf{A_1}$ and $\mathbf{B_1}$ in Equation (3) are obtained and their expressions are given in Appendix 2. In this model, $\mathbf{e_1}$ is an (18×1) vector and represents the fixture induced error. The quality characteristic of interest is the orientation deviation of feature f_1; therefore, the parameters of interest in $\mathbf{q_{f_1}} = [x\ y\ z\ e_1\ e_2\ e_3]^T$ will only be the two rotational parameters $[e_1, e_2]$ because $[x, y, z]$ represents the location deviation which is of no interest here and e_3, which represents the rotation around z-axis, makes no difference to the feature plane no matter what value it takes. To obtain the worst case deviations, the following procedure is applied: first, the methodology proposed in this paper is used to obtain the possible deviations of datum A, on which a perpendicularity characteristic is defined, expressed as a differential motion vector $\mathbf{q_A}$:

$$\mathbf{q_A} = \begin{bmatrix} -0.02 & 0.02 & 0 \\ -0.02 & 0 & 0.02 \\ -0.2 & 0.3 & 0.9 \end{bmatrix} \begin{bmatrix} \alpha_1 \\ \alpha_2 \\ \alpha_3 \end{bmatrix}, \quad \alpha_4 = -\alpha_1 + \alpha_2 + \alpha_3, \tag{12}$$

where α_1, α_2, α_3, and α_4 are parameters constraining the deviation of points ${}^0P_1$, ${}^0P_2$, ${}^0P_3$, and ${}^0P_4$, respectively, and satisfying $-0.05 \le \alpha_i \le 0.05$, $i = 1, \ldots, 4$.

Table 4. 3DCS and model predicted results (1×10^{-3} rad).

Component	DCS min.	Model min.	% error	DCS max.	Model max.	% error
e_1	−4.99996	−4.99989	0.001%	4.99996	4.99989	0.001%
e_2	−4.30938	−4.31009	0.02%	4.30939	4.31009	0.02%

Then, the possible deviations of datum C, constrained by an angularity characteristic, are obtained in terms of a differential motion vector $\mathbf{q_C}$:

$$\mathbf{q_C} = \begin{bmatrix} -0.01 & 0 & 0.01 & -0.02 & 0.02 & 0 \\ -0.02 & 0.02 & 0 & -0.0115 & 0 & 0.0115 \\ -0.9056 & 1.1556 & 0.25 & 0 & -0.5 & -0.5 \end{bmatrix} \cdot \left[\begin{bmatrix} \alpha_1 \\ \alpha_2 \\ \alpha_3 \end{bmatrix}^T \quad \begin{bmatrix} \alpha_5 \\ \alpha_6 \\ \alpha_7 \end{bmatrix}^T \right]^T$$

$$\alpha_4 = -\alpha_1 + \alpha_2 + \alpha_3$$

$$\alpha_8 = -0.4208 \cdot \alpha_1 - 0.5832 \cdot \alpha_2 - \alpha_5 + \alpha_6 + \alpha_7, \tag{13}$$

where α_5, α_6, α_7, and α_8 are parameters constraining the deviation of points ${}^0P_5$, ${}^0P_6$, ${}^0P_7$, and ${}^0P_8$, respectively, and satisfying $-0.1 \le \alpha_i \le 0.1$, $i = 5, \ldots, 8$.

Finally, the SoV model is used to determine the deviation of feature f_1 as a function of the deviations of the machining datums C and A. Assuming that datum E is perfect (e.g., $\mathbf{q_E} = \mathbf{0}$) and that there is no fixture induced error (e.g., $\mathbf{e_k} = \mathbf{0}$ in Equation (3)), the deviation of feature f_1 ($\mathbf{q_{f_1}}$) is determined as a function of parameters α_i, $i = 1, \ldots, 8$. The extremes of the orientation parameters $[e_1, e_2]$ in $\mathbf{q_{f_1}}$, corresponding physically to worst case realisations of the feature, are then determined.

4.3 *Results*

The machining operation presented in Figure 11 has been modelled using 3DCS, a commercial tolerance simulation software widely used in practice that allows dimensional variation analysis. 3DCS allows the definition of GD&T characteristics on CAD features and simulates the deviation of these features using Monte Carlo simulation assuming a normal distribution of the feature deviation within the tolerance zone. For each simulation executed by the software, a realisation of the feature constrained by the GD&T characteristic is determined. The output measured using 3DCS corresponds to the deviation from nominal of the controlled feature with respect to the PCS. The extremums of the deviation found after 50,000 simulations are then compared with the values determined following the procedure proposed in this paper. Table 4 gathers the comparison results between the two models.

The comparison results in Table 4 indicate that the difference between the 3DCS prediction and the model prediction is very small. The 3DCS results are from numerical simulations based on the non-linear relationships, whereas the proposed methodology is based on linear equations, assuming that the deviations of the feature are small (e.g., the value of the GD&T characteristic is small compared to the size of the controlled feature). The results show that the linearisation error is quite small (below 0.1%) in these cases.

5. Conclusion

The mathematical formulation of GD&T requirements is a complicated topic. In this paper, an analytical derivation was developed to describe the deviations of the features in terms of a differential motion vector controlled by GD&T characteristics. The derivation has been shown for positional, orientation and form tolerances. It has been applied to specific GD&T characteristics but remains very general nonetheless. A similar logic can be applied to other GD&T characteristics including the material condition modifiers. This formulation allows for the determination of the worst case deviations of the feature given a GD&T specification in different directions or orientations using homogeneous transformations. This translation of GD&T characteristics formalised mathematically using matrices creates an interface between variation propagation (SoV) models and GD&T standards.

Using the state space model with this interface, variation simulation can be easily conducted with given initial conditions. The model developed in this paper allows practitioners to specify and analyse the workpiece tolerances in terms of GD&T. It is valuable to evaluate a process since it gives an analytical representation of a design specification defined in the early design stage as well as product dimensional quality measured in-line. Other GD&T characteristics such as the profile of a surface and the inclusion of material condition modifiers will be studied in the future.

When the error is represented by its statistical distribution rather than a fixed value, e.g., the location of a loose fixture locator can be modelled by a normal distribution around its nominal position, the distribution of the feature deviation from its nominal position can be investigated based on the same model in Equation (3). Therefore, the current work can be linked with the statistical tolerancing research area.

Acknowledgements

The authors gratefully acknowledge the financial support of the National Science Foundation award DMI-033147, UK EPSRC Star Award EP/E044506/1 and the NIST Advanced Technology Program (ATP Cooperative Agreement # 70NANB3H3054). The authors also appreciate the fruitful discussion with Mr Ramesh Kumar and Dr Ying Zhou from Dimensional Control Systems, Inc.

References

ASME, 1994. *Dimensioning and tolerancing: engineering drawing and related documentation practices*. New York: American Society of Mechanical Engineers.

Bourdet, P., *et al*., 1996. The concept of the small displacement torsor in metrology. *In*: P. Ciarlin, ed. *Advanced mathematical tools in metrology II*. River Edge, NJ: World Scientific Publishing, 110–122.

Ceglarek, D., *et al*., 2004. Time-based competition in manufacturing stream-of-variation analysis (SOVA) methodology review. *International Journal of Flexible Manufacturing Systems*, 16 (1), 11–44.

Craig, J.J., 1989. *Introduction to robotics: mechanics and control*. 2nd ed. Reading, MA: Addison-Wesley.

Desrochers, A. and Riviere, A., 1997. A matrix approach to the representation of tolerance zones and clearances. *International Journal of Advanced Manufacturing Technology*, 13 (9), 630–636.

Desrochers, A., 1999. Modeling three-dimensional tolerance zones using screw parameters. *In*: M.A. Ganter, ed. (*CD-ROM*) *Proceedings of the ASME 25th design automation conference*, 12–15 September Las Vegas, Nevada, paper #DETC99/DAC-8587, 895–903.

Desrochers, A., Ghie, W., and Laperrière, L., 2003. Application of a unified Jacobian-torsor model for tolerance analysis. *Journal of Computer and Information Science and Engineering – Transaction of the ASME*, 3 (1), 2–14.

Ding, Y., Ceglarek, D., and Shi, J. 2000. Modeling and diagnosis of multistage manufacturing processes: part i: state space model. *In*: S.Y. Liang, ed. *Proceedings of the 2000 Japan/USA symposium on flexible automation*, 23–26 July Ann Arbor, Michigan, paper #2000JUSFA-13146, 233–240.

Ding, Y., Ceglarek, D., and Shi, J., 2002a. Fault diagnosis of multistage manufacturing processes by using state space approach. *Journal of Manufacturing Science and Engineering – Transactions of ASME*, 124 (2), 313–322.

Ding, Y., Ceglarek, D., and Shi, J., 2002b. Design evaluation of multi-station assembly processes by using state space approach. *Journal of Mechanical Design*, 124 (3), 408–418.

Ding, Y., Zhou, S., and Chen, Y., 2005a. A comparison of process variation estimators for in-process dimensional measurements and control. *Journal of Dynamic Systems Measurement and Control – Transactions of ASME*, 127 (1), 69–79.

Ding, Y., *et al*., 2005b. Process-oriented tolerancing for multi-station assembly systems. *IIE Transactions*, 37 (6), 493–508.

Djurdjanovic, D. and Ni, J., 2001. Linear state space modeling of dimensional machining errors. *Transaction of NAMRI/SME*, 29 (1), 541–548.

Henzold, G., 1995. *Handbook of geometrical tolerancing: design, manufacturing, and inspection*. New York: Wiley.

Hong, Y.S. and Chang, T.-C., 2002. A comprehensive review of tolerancing research. *International Journal of Production Research*, 40 (11), 2425–2459.

Huang, Q., Zhou, N., and Shi, J. 2000. Stream of variation modeling and diagnosis of multi-station machining processes. *In*: R.J. Furness, ed. *Proceedings of the international mechanical engineering* 2000 *ASME congress & exposition*, 5–10 November Orlando, Florida, Vol. 11, 81–88.

Huang, W., *et al*., 2007a. Stream-of-variation modeling I: A generic 3D variation model for rigid body assembly in single station assembly processes. *ASME Trans on Journal of Manufacturing Science and Engineering*, 129 (4), 821–831.

Huang, W., *et al*., 2007b. Stream-of-variation modeling II: A generic 3D variation model for rigid body assembly in multi-station assembly processes. *ASME Trans on Journal of Manufacturing Science and Engineering*, 129 (4), 832–842.

Jin, J. and Shi, J., 1999. State space modeling of sheet metal assembly for dimensional control. *Journal of Manufacturing Science and Engineering – Transactions of ASME*, 121 (4), 756–762.

Kong, Z., *et al*., 2005. Multiple fault diagnosis method in multi-station assembly processes using orthogonal diagonalisation analysis. *Proceedings of the ASME 2005 International Mechanics Engineering Congress and Exposition*, 5–11 November, Orlando, USA, 1201–1212.

Laperrière, L., and Lafond, P. 1998. Modeling dispersions affecting pre-defined functional requirements of mechanical assemblies using Jacobian transforms. *In*: J.L. Batoz, ed. *Proceedings of the 2nd integrated design and manufacturing in mechanical engineering* (*IDMME*) *conference*, 28–29 April, Charlotte, NC, USA, 381–388.

Laperrière, L., Ghie, W., and Desrochers, A. 2003. Projection of torsors: a necessary step for tolerance analysis using the unified Jacobian-torsor model. *In*: *Proceedings of 8th CIRP international seminar on computer aided tolerancing*, 14–23.

Loose, J.-P., Zhou, S., and Ceglarek, D., 2007. Kinematic analysis of dimensional variation propagation for multistage machining processes with general fixture layout. *IEEE Transactions on Automation Science and Engineering*, 4 (2), 141–152.

Pasupathy, T.M.K, Morse, E.P., and Wilhelm, R.G., 2003. A survey of mathematical methods for the construction of geometric tolerance zones. *Journal of Computing and Information Science in Engineering – ASME Transactions*, 3 (1), 64–75.

Paul, R.P., 1981. *Robot manipulators: mathematics, programming, and control: the computer control of robot manipulators*. Cambridge, MA: MIT Press.

Requicha, A., 1983. Toward a theory of geometric tolerancing. *International Journal of Robotics Research*, 2 (4), 45–60.

Rivest, L., Fortin, C., and Morel, C., 1994. Tolerancing a solid model with a kinematic formulation. *Computer-Aided Design*, 26 (6), 465–476.

Salomons, O.W., *et al*., 1996. A computer aided tolerancing tool II: tolerance analysis. *Computer in Industry*, 31 (2), 175–186.

Shi, J., 2007. Stream of variation modeling and analysis for multistage manufacturing processes. Boca Raton, FL: CRC Press/Taylor and Francis.

Teissandier, D., Couétard, Y., and Gérard, A., 1999. A computer aided tolerancing model: proportioned assembly clearance volume. *Computer-Aided Design*, 31 (13), 805–817.

Zhou, S., Huang, Q., and Shi, J., 2003. State space modeling of dimensional variation propagation in multistage machining process using differential motion vectors. *IEEE Transactions on Robotics and Automation*, 19 (2), 296–309.

Zhou, S., Chen, Y., and Shi, J., 2004. Statistical estimation and testing for variation root-cause identification of multistage manufacturing processes. *IEEE Transactions on Automation Science and Engineering*, 1 (1), 73–83.

Appendix 1

Proof to Lemma 1: *Define* $[{}^0\mathbf{P_{i,true}}]_{\mathrm{LCS_K}}$ *and* $[{}^0\mathbf{P_i}]_{{}^0\mathrm{LCS_K}}$ *as the coordinates of* ${}^0\mathrm{P}_{i,\mathrm{true}}$ *in* $\mathrm{LCS_K}$ *and* ${}^0\mathrm{P}_i$ *in* ${}^0\mathrm{LCS_K}$, *respectively. Because* ${}^0\mathrm{P}_{i,\mathrm{true}}$ *has the same coordinates in* $\mathrm{LCS_K}$ *as* ${}^0\mathrm{P}_i$ *in* ${}^0\mathrm{LCS_K}$, *we have*, $[{}^0\mathbf{P_{i,true}}]_{\mathrm{LCS_K}} = [{}^0\mathbf{P_i}]_{{}^0\mathrm{LCS_K}}$. *However, it is known that* $[{}^0\mathbf{P_i}]_{{}^0\mathrm{LCS_K}} = {}^0\mathbf{H_K^{-1}} \cdot [{}^0\mathbf{P_i^T} \quad 1]^T$ *and thus we have* $[{}^0\mathbf{P_{i,true}}]_{\mathrm{LCS_K}} = {}^0\mathbf{H_K^{-1}} \cdot [{}^0\mathbf{P_i^T} \quad 1]^T$. *Further, a left multiplication of* $\mathbf{H_i}$ *will deviate* ${}^0\mathrm{P}_{i,\mathrm{true}}$ *along the normal direction of feature* K *in* $\mathrm{LCS_K}$. *Finally, the left multiplication by* ${}^0\mathbf{H_K} \cdot \mathbf{H(q_K)}$ *translates the coordinates in* $\mathrm{LCS_K}$ *into the coordinates in* PCS.

Appendix 2

$$
\mathbf{A}_1 = \mathbf{F}_3 \cdot
\begin{bmatrix}
0 & 0 & 4.448 & 120.391 & 41.705 & 0 & 0 & 0 & -7.272 & -118.09 & 68.180 & 0 \\
0 & 0 & -2.568 & -69.508 & -24.078 & 0 & 0 & 0 & 4.199 & 68.179 & -39.364 & 0 \\
0 & 0 & 0.792 & 21.435 & 7.425 & 0 & 0 & 0 & -2.295 & -37.263 & 21.514 & 0 \\
0 & 0 & -0.060 & -1.615 & -0.559 & 0 & 0 & 0 & 0.083 & 1.346 & -0.777 & 0 \\
0 & 0 & -0.019 & -0.511 & -0.177 & 0 & 0 & 0 & 0.005 & 0.089 & -0.051 & 0 \\
0 & 0 & 0.122 & 3.300 & 1.143 & 0 & 0 & 0 & -0.199 & -3.237 & 1.869 & 0
\end{bmatrix} \cdots
$$

$$
\cdots
\begin{bmatrix}
0 & 0 & 2.824 & 88.901 & -162.539 & 0 & -2.106 & 0 & 3.648 & -45.60 & -127.682 & -26.33 \\
0 & 0 & -1.630 & -51.327 & 93.842 & 0 & 0.927 & 0 & -1.606 & 20.078 & 56.217 & 11.592 \\
0 & 0 & 0.503 & 15.828 & -28.939 & 0 & 0 & 0 & 0 & 0 & 0 & 0 \\
0 & 0 & -0.023 & -0.731 & 1.337 & 0 & 0 & 0 & 0 & 0 & 0 & 0 \\
0 & 0 & 0.013 & 0.422 & -0.772 & 0 & 0 & 0 & 0 & 0 & 0 & 0 \\
0 & 0 & 0.077 & 2.437 & -4.455 & 0 & -0.577 & 0 & 0.1 & -1.25 & -3.5 & -0.722
\end{bmatrix} \cdots
$$

$$
\cdots
\begin{bmatrix}
2.106 & 0 & -3.648 & -45.60 & 91.201 & -26.328 & -1 & 0 & 0 & 0 & 0 & 36.481 \\
-1.505 & 0 & 2.606 & 32.578 & -65.155 & 18.809 & 0.577 & 0 & 0 & 0 & 0 & -21.062 \\
0 & 0 & 0 & 0 & 0 & 0 & 0 & 0 & 0 & 0 & 0 & 0 \\
0 & 0 & 0 & 0 & 0 & 0 & 0 & 0 & 0 & 0 & 0 & 0 \\
0 & 0 & 0 & 0 & 0 & 0 & 0 & 0 & 0 & 0 & 0 & 0 \\
0.0577 & 0 & -0.1 & -1.25 & 2.5 & -0.722 & 0 & 0 & 0 & 0 & 0 & 0
\end{bmatrix}
$$

$$\mathbf{B}_1 = \mathbf{F}_3 \cdot \begin{bmatrix} 0 & 0 & -4.448 & 0 & 0 & 7.272 & 0 & 0 & -2.824 & \\ 0 & 0 & 2.568 & 0 & 0 & -4.199 & 0 & 0 & 1.630 & \\ 0 & 0 & -0.792 & 0 & 0 & 2.295 & 0 & 0 & -0.503 & \\ 0 & 0 & 0.060 & 0 & 0 & -0.083 & 0 & 0 & 0.023 & \cdots \\ 0 & 0 & 0.019 & 0 & 0 & -0.005 & 0 & 0 & -0.013 & \\ 0 & 0 & -0.122 & 0 & 0 & 0.199 & 0 & 0 & -0.077 & \end{bmatrix}$$

$$\cdots \begin{bmatrix} 2.106 & 3.648 & 0 & -2.106 & -3.648 & 0 & 0 & 1 & 0 \\ -0.927 & -1.606 & 0 & 1.505 & 2.606 & 0 & 0 & -0.577 & 0 \\ 0 & 0 & 0 & 0 & 0 & 0 & 0 & 0 & 0 \\ 0 & 0 & 0 & 0 & 0 & 0 & 0 & 0 & 0 \\ 0 & 0 & 0 & 0 & 0 & 0 & 0 & 0 & 0 \\ 0.058 & 0.1 & 0 & -0.057 & -0.1 & 0 & 0 & 0 & 0 \end{bmatrix}$$

$$\mathbf{F}_3 = \begin{bmatrix} -1 & 0 & 0 & 0 & -25 & 30.3109 \\ 0 & -1 & 0 & 25 & 0 & -37.5 \\ 0 & 0 & -1 & -30.3109 & 37.5 & 0 \\ 0 & 0 & 0 & -1 & 0 & 0 \\ 0 & 0 & 0 & 0 & -1 & 0 \\ 0 & 0 & 0 & 0 & 0 & -1 \end{bmatrix}.$$